1 **Insights into the Absence of Lymphoma Despite Fulminant Epstein-Barr Virus Infection in**

2 **Patients with XIAP Deficiency**

3

4 Yizhe Sun[1,2], Janet Chou[3], Kevin Dong[4], Steven P. Gygi[4] and Benjamin E. Gewurz[1,2,5,6,*]

5

6 [1]Division of Infectious Diseases, Department of Medicine, Brigham and Women's Hospital,

7 Boston, Massachusetts, United States of America.

8 [2]Harvard Program in Virology, Harvard Medical School, Boston, Massachusetts, United States

9 of America.

10 [3]Division of Immunology, Department of Pediatrics Harvard Medical School, Boston Children's

11 Hospital, Boston, Massachusetts, USA.

12 [4]Department of Cell Biology, Harvard Medical School, Boston, Massachusetts, United States

13 [5]Center for Integrated Solutions for Infectious Diseases, Broad Institute of Harvard and MIT,

14 Cambridge, Massachusetts, United States of America.

15 [6]Department of Microbiology, Harvard Medical School, Boston, Massachusetts, United States of

16 America.

17

18 *181 Longwood Ave, Boston, Massachusetts 02115, USA; email: bgewurz@bwh.harvard.edu;

19 phone number: 617-525-4282

20 Text word count: 3980

21 Abstract word count: 241

22 Figure/table count: 6

23 Reference count: 54

24

25 Short title for the running head: XIAP modulates EBV-driven B-cell transformation.

26

Key points

1. XIAP loss-of-function markedly impairs EBV+ B-cells outgrowth over the first week post-infection, particularly in the presence of IFN-γ.

2. XIAP mutation impedes EBV-driven B-cell transformation by potentiating p53-driven caspase activation and apoptosis.

Abstract

X-linked Lymphoproliferative Syndromes (XLP), which arise from mutations in the *SH2D1A* or *XIAP* genes, are characterized by the inability to control Epstein-Barr Virus (EBV) infection. While primary EBV infection triggers severe diseases in each, lymphomas occur at high rates with XLP-1 but not with XLP-2. Why XLP-2 patients are apparently protected from EBV-driven lymphomagenesis, in contrast to all other described congenital conditions that result in heightened susceptibility to EBV, remains a key open question. To gain insights, we cross-compared newly EBV infected versus immune stimulated B-cells from XLP-2 patients or upon XIAP CRISPR knockout, relative to healthy controls. XIAP perturbation impeded outgrowth of newly EBV-infected primary human B-cells, though had no impact on proliferation of B-cells stimulated by CD40 ligand and interleukin-21 or upon established EBV-immortalized lymphoblastoid cell lines (LCLs). B-cells from XLP-2 patients or in which XIAP was depleted by CRISPR editing exhibited a markedly lower EBV transformation efficiency than healthy control B-cells. Mechanistically, nascent EBV infection activated p53-mediated apoptosis signaling, whose effects on transforming B-cell death were counteracted by XIAP. In the absence of XIAP, EBV infection triggered high rates of apoptosis, not seen with CD40L/IL-21 stimulation. Moreover, inflammatory cytokines are present at high levels in XLP-2 patient serum with fulminant EBV infection, which heightened apoptosis induction in newly EBV-infected cells. These findings highlight the crucial role of XIAP in supporting early stages of EBV-driven B-cell immortalization and provide insights into the absence of EBV+ lymphoma in XLP-2 patients.

Introduction

EBV persistently infects more than 90% of the global population and contributes to over 200,000 cancers per year [1-3]. While acute EBV infection is controlled by immunocompetent hosts and typically results in subclinical disease, EBV is nonetheless a major driver of pathology in hosts with primary or acquired immunodeficiency, in particular lymphoproliferative disease [4-8]. EBV is associated with 200,000 cancers per year, including lymphomas, gastric and nasopharyngeal carcinoma [9]. Defects in anti-EBV immunity increase rates of multiple EBV-associated lymphomas including Burkitt, Hodgkin and immunoblastic lymphomas [5,7,10].

Immune control over EBV is primarily mediated by T-cell responses, particularly CD8$^+$ cytotoxic T lymphocytes, which target virus-infected cells. Natural killer (NK) cells and antibodies also play crucial roles in regulating EBV activity[11]. The importance of these immune mechanisms is underscored by the severe outcomes observed in individuals with compromised immunity, such as those with X-linked lymphoproliferative syndromes (XLP)[11]. In these cases, defects in immune signaling pathways can lead to uncontrolled viral proliferation and associated complications, highlighting the critical balance between EBV and host immune responses.

Two rare congenital XLP syndromes have been described, which share in common extreme susceptibility to EBV, frequently resulting in fulminant infectious mononucleosis, dysgammaglobulinemia and hemophagocytic lymphohistiocytosis (HLH). HLH is a T-cell and macrophage hyperactivation state [12-14]. XLP-1 is caused by loss-of-function mutations in *SH2D1A*, which encodes the protein 128 amino acid SH2-domain containing signaling lymphocyte activation molecule (SLAM)–associated protein (SAP) (MIM no. 308240). SAP controls signaling downstream of SLAM family receptors, including CD150, CD229, 2B4, CD84 and NTB-A [15,16]. XLP-2 instead arises from congenital mutations of the X-linked inhibitor of apoptosis (XIAP, also termed BIRC4; MIM no. 300635), a 497-amino acid member of the inhibitor of apoptosis protein (IAP) family that serves as a central regulator of apoptotic cell

78 death by inhibiting caspases 3 and 7 [15-19]. XIAP has additional roles in many other pathways [20].

79 Each XLP syndrome is characterized by markedly elevated EBV viral loads [21,22], which trigger

80 severe infectious mononucleosis, HLH and a range of hematological dyscrasias. While rates of

81 HLH and splenomegaly are higher with XLP-2, there are no reported cases of EBV-associated

82 lymphoproliferative disease in this syndrome. This stands in contradistinction to essentially all

83 other primary immunodeficiency syndromes manifest by susceptibility to EBV [21,23]. Much

84 remains to be learned about why *SH2D1A* and *XIAP* mutations cause XLP syndromes, but each

85 is associated with defects in T and NK cell responses, including the absence of natural killer T-

86 cells [7].

87 A notable difference between SAP and XIAP is their tropism. While SAP is expressed primarily

88 in NK, NKT and T cells, XIAP is ubiquitously expressed in all cell types [21]. This disparity

89 suggests that the lack of B-cell malignancies in XLP-2 may be attributed to intrinsic factors

90 within EBV-infected B-cells themselves, rather than solely to differences in immune cell function.

91 Gene expression analysis highlighted elevated levels of the tumor suppressor cell adhesion

92 molecule 1 (CADM1) in XIAP-deficient B-cells infected by EBV [24], which has been implicated in

93 NF-kB activation in B-cells infected by the gamma-herpesvirus Kaposi's Sarcoma Associated

94 Herpesvirus [25].

95 Here, we sought to test the role of XIAP in EBV-driven lymphomagenesis. We found that the

96 knockout or mutation of *XIAP* in primary B-cells impacted the EBV-driven proliferation of newly

97 infected B-cells, leading to reduced efficiency in B-cell transformation. We provide evidence that

98 XIAP supports newly EBV-infected primary B-cell survival, which counteracted upregulation of

99 p53-related apoptosis signaling triggered by EBV infection. B-cell intrinsic XIAP deficiency

100 elevated the apoptosis frequency at early timepoints of EBV-mediated B-cell immortalization but

101 not in cells stimulated by CD40-ligand (CD40L) and interleukin-4 (IL-4), exacerbated by the

102 presence of inflammatory cytokines.

103 **Materials and methods**

104 Cell cultures and Chemical compounds

105 Cells were cultured following the vendor's instructions. Details are in the supplemental materials

106 and methods. Chemical compounds used in the study are listed in the supplemental materials

107 and methods.

108 Primary Human B cells

109 Leukocyte fractions that were discarded and de-identified, originating from platelet donations,

110 were obtained from the Brigham and Women's Hospital Blood Bank. These fractions were

111 utilized for the isolation of primary human B cells following our Institutional Review Board-

112 approved protocol. Venous blood of XLP2 patients and corresponding controls were obtained

113 from Boston Children's Hospital. PBMCs were isolated using Lymphopre Density Gradient

114 Medium (Stem Cell Technologies), and primary B cells were subsequently isolated by negative

115 selection using RosetteSep Human B Cell Enrichment and EasySep Human B cell enrichment

116 kits (Stem Cell Technologies), according to the manufacturers' protocols. Cells were cultured in

117 RPMI-1640 medium with 10% FBS.

118 EBV production

119 For production of Akata EBV, Akata EBV+ cells were resuspended in FBS-free RPMI-1640 at a

120 concentration of 2-3×10^6 cells per ml and treated by 0.3% Polyclonal Rabbit Anti-Human IgG

121 (Agilent) for 6 hours. Cells were cultured in RPMI-1640 with 4% FBS for 3 more days, and the

122 virus-containing supernatants were collected by ultracentrifugation and filtration through a 0.45

123 μm filter. The viral titer was determined by EBV transformation assay as described below.

124 EBV transformation assay

125   Purified human primary B cells were seeded into a 96 well plate at 50000 cells per well. The

126   stock of Akata EBV was diluted ten-fold in order, and 100 μL of virus dilution was added to each

127   well. The cells were maintained in RPMI-1640 with 10% FBS at 37°C. After 4 weeks of

128   incubation, the proportion of wells with B cell outgrowth was scored. A transforming unit per well

129   was defined as the virus quantity necessary for achieving B cell outgrowth in 50% of wells. The

130   multiple of infection (MOI) was determined by dividing the Transforming Unit by the cell number.

131   CRISPR/Cas9 editing

132   For cell lines with stable Cas9 expression, sgRNA sequences from Broad Institute Brunello

133   library were used. sgRNA oligos were cloned into the pLentiGuide-Puro vector (Addgene

134   plasmid #52963, a gift from Feng Zhang), and used for lentivirus production in HEK293T cells.

135   After 2 rounds of transduction performed at 48 and 72 hours post plasmids transfection, cells

136   were selected by 3 μg/ml puromycin for more than 4 days.

137   For CRISPR/Cas9 editing in primary B cells, Cas9 RNA complexes were transduced into the

138   cells with electroporation. In brief, crRNA targeting XIAP was selected using Alt-R Predesigned

139   Cas9 crRNA Selection Tool from Integrated DNA Technologies. TracrRNA and Cas9 Nuclease

140   V3 were also obtained from Integrated DNA Technologies. The crRNA and tracrRNA were

141   annealed to form the duplex and incubated with Cas9 for 20 minutes. Then the cells were mixed

142   with the RNP complexes, and electroporated using the Neon NxT Electroporation System at

143   1700V, 20ms and 2 pulses. sgRNA sequences were listed in Table S1.

Results

XIAP supports the outgrowth of newly EBV-infected primary human B-cells.

EBV transforms primary human B-cells into immortalized, continuously proliferating

lymphoblastoid cell lines (LCLs), which serves as a major model for EBV lymphomagenesis. To

characterize how XIAP deficiency affects EBV-mediated B-cell immortalization, we utilized

CRISPR-Cas9 technology to knockout (KO) *XIAP* in primary B-cells isolated from healthy

donors (Figure 1A). FACS analysis indicated that Cas9/single guide RNA (sgRNA)

ribonucleoprotein complexes (RNP) were successfully delivered to >50% of B-cells (Figure

S1A), and immunoblot analysis confirmed depletion of XIAP expression across the bulk

population (Figure 1B).

Control versus XIAP depleted B-cells were infected with EBV, or for cross-comparison,

stimulated by CD40L and IL-21, a combination which efficiently drives B-cell proliferation [26].

XIAP editing did not significantly alter EBV infection efficiency, as judged by an EBV genomic

green fluorescence protein (GFP) reporter that can be used to mark infected B-cells (Figure

1C). However, growth curve analysis highlighted that *XIAP* editing markedly reduced the

efficiency of EBV-driven primary B-cell outgrowth. Intriguingly, XIAP KO did not significantly alter

proliferation of CD40L/IL-21 treated cells, suggesting an EBV-specific, B-cell intrinsic phenotype

(Figure 1D). Our CRISPR editing only depleted XIAP in a subset of B-cells, likely due to the

inability to deliver Cas9 RNPs across the population. Consistent with a growth advantage for

XIAP-expressing cells, immunoblot analysis highlighted that there was a selection against XIAP

deficiency evident by day 14 post-infection, with similar XIAP levels present in control vs XIAP

edited populations, in contrast to earlier timepoints (Figure 1E).

To further characterize a potential XIAP role in support of early EBV-mediated B-cell outgrowth,

we treated newly infected versus CD40L/IL-21 stimulated B-cells with the small-molecule XIAP

7

168   antagonist embelin [27]. Consistent with the *XIAP* KO phenotype, embelin significantly impeded

169   EBV-driven but not CD40L/IL21-induced B-cell outgrowth (Figure 1F). Taken together, these

170   results indicate that XIAP plays a B-cell intrinsic role in EBV, but not CD40L/IL-21 driven

171   proliferation. By contrast, consistent with prior reports [24], XIAP KO or inhibition by embelin in

172   established LCLs failed to significantly alter proliferation of either GM12878 or GM15892 LCLs,

173   despite excellent efficiency of CRISPR editing (Figure 1G-H, S1B-C), suggesting that XIAP may

174   specifically play a critical role at an early stage of EBV-mediated B-cell transformation. In

175   support of this hypothesis, early administration of embelin impaired EBV-driven outgrowth, but

176   its impact was non-significant when started at 7 days post-EBV infection or at later timepoints

177   (Figure 1I). Collectively, these findings suggest that XIAP plays a critical role in support of EBV-

178   infected B-cell transformation within the first week of infection.

179

180   **Newly EBV-infected but not CD40L/IL-21 driven proliferation is impaired in XLP-2 B-cells.**

181   We next characterized effects of XIAP deficiency on early EBV-mediated B-cell outgrowth in

182   primary B-cells from XLP-2 patients versus from healthy controls. XLP-2 patients 1 and 2, who

183   are brothers, possess an XIAP missense variant (NP_001158.2: p.Ser421Asn) that

184   compromises XIAP function (Figure 2A) [28]. Venous blood was collected from three healthy

185   donors on the same day (Control 1-3). B-cells were purified by negative selection and infected

186   by EBV or stimulated by CD40L/IL-21. Similar to our XIAP CRISPR analyses, proliferation of

187   XLP-2 cells was diminished over the first week of infection relative to healthy controls (Figure

188   2B). By contrast, XLP-2 and control B-cells proliferated similarly in response to CD40L and IL21-

189   treatment (Figure 2C). We observed similar effects with B-cells from two additional XLP-2

190   patients (Patients 3 and 4) who possess an XIAP nonsense variant (NP_001158.2: p.Arg49*)

191   (Figure S2A-C). Consistent with a key early but not late XIAP role in support of EBV-mediated

8

192 transformation, LCLs established from both XLP-2 patients and from controls proliferated at

193 similar rates (Figure 2D).

194 To further characterize *XLP-2* mutation effects, we conducted transformation assays, in which

195 serial dilutions of EBV are added to primary B-cells, and the percentage of wells with cellular

196 outgrowth are scored at 4 weeks post-infection (Figure 2E). Consistent with our growth curve

197 phenotypes, *XIAP* mutation significantly reduced EBV B-cell transformation efficiency (Figure

198 2F). Together, these findings demonstrate the limited extent of EBV-induced B-cell

199 transformation in XLP2 patients.

200

201 **XIAP plays key anti-apoptosis roles in newly-EBV infected B-cells.**

202 To explore the mechanism by which XIAP supports EBV but not CD40/IL-21-driven B-cell

203 outgrowth, we tested the effects of XIAP depletion on growth versus survival at early times post-

204 EBV infection. Interestingly, CRISPR XIAP editing significantly impaired proliferation of EBV

205 infected but not CD40L/IL-21 stimulated cells (Figure 3A-3B). Furthermore, FACS analysis of 7-

206 AAD vital dye uptake revealed an increased percentage of cell death in XIAP edited and EBV-

207 infected, but not CD40L/IL-21 stimulated B-cells (Figure 3C).

208 We hypothesized that XIAP deficiency might sensitize EBV-infected cells to apoptotic cell death,

209 given XIAP's ability to block executioner caspase activity, including caspases 3 and 7 [29]. In

210 support, caspase 3 and 7 activity was significantly elevated in XIAP edited cells on day 4 post-

211 EBV infection but not at the same timepoint of CD40L/IL-21 stimulation (Figure 3D). Caspase

212 3/7 activity was similarly elevated at Day 4 post-EBV-infection but not CD40L/IL-21 stimulation

213 of XLP-2 patient primary B-cells (Figure 3E). We therefore tested whether caspase activity was

214 necessary for EBV-triggered cell death of XIAP-deficient B-cells. The pan-caspase inhibitor

215 zVAD-Fmk significantly inhibited caspase 3/7 activity and blocked EBV-driven cell death of XIAP

9

216   edited cells (Figure 3F-G). zVAD-Fmk also significantly increased the outgrowth of EBV-infected

217   *XIAP* CRISPR edited cells (Figure 3H). These results suggest that EBV infection drives an

218   apoptotic stimulus within the first week of primary B-cell infection, a period in which EBV drives

219   Burkitt-like hyperproliferation [30-32], and that XIAP anti-caspase activity is critical to overcome

220   EBV-triggered caspase activity in support viral mediated B-cell transformation.

221

EBV activates p53 induced apoptosis signaling.

223   We next aimed to decipher the mechanism behind XIAP's differential impact on EBV-infected

224   but not CD40L/IL-21 proliferation. To gain insights, we performed systematic transcriptomic and

225   whole cell proteomic analyses of XLP-2 versus healthy control B-cells at Day 7 post-EBV

226   infection or CD40L/IL-21 stimulation. This analysis highlighted that EBV infection upregulated

227   expression of P53 (encoded by *TP53*) relative to levels in CD40L/IL-21 stimulated cells. EBV

228   also altered expression levels of multiple apoptosis pathway components, increasing levels of

229   the pro-apoptotic BAX, NOXA (encoded by PMAIP1) and PUMA (encoded by BBC3) in both

230   control and XLP2 patient B-cells (Figure 4A and 4B and Table S2 and S3). Intriguingly, many of

231   these genes are associated with the p53 signaling pathway. Notably, these data are consistent

232   with prior transcriptomic and proteomic analyses [30,33] of peripheral blood B-cell EBV infection,

233   which identified that levels of TP53 and BAX peak at day 4 post-EBV infection and then

234   gradually decline (Figure 4C).

235   P53, as well as multiple p53-upregulated pro-apoptotic proteins can induce expression of the

236   pro-apoptosis BCL-2 family member BAX [34,35] (Figure 4D). We therefore tested whether the

237   small molecule allosteric BAX inhibitor BAI1 [36] could suppress apoptosis induction in newly

238   EBV-infected XIAP deficient cells. Interestingly, BAX blockade by BAI significantly diminished

239   EBV-driven caspase 3/7 activity in XIAP deficient cells (Figure 4E). Similarly, BAI significantly

240   restored EBV-mediated outgrowth of CRISPR XIAP-edited B-cells (Figure 4F). In further support

241   of a key p53 role, p53 inhibition by pifithrin-α [37] also significantly inhibited EBV-driven caspase

242   3/7activity in XIAP depleted primary B-cells (Figure 4G). These results suggest that EBV

243   upregulates p53-driven BAX activation, whose activation of downstream caspase signaling

244   necessitates XIAP to inhibit apoptosis.

245

246   **XIAP in EBV transformed cells renders sensitivity to inflammatory cytokines.**

247   While the above experiments indicate a role for XIAP in protecting newly EBV infected cells

248   from apoptosis, a subset of EBV+ B-cells survive and can be immortalized, raising the question

249   of why this does not apparently lead to lymphoma in XLP-2 patients. One hypothesis is, other

250   factors in vivo may further influence the transformation of EBV-infected XIAP deficient cells. To

251   test this hypothesis, we first treated peripheral blood mononuclear cells (PBMC) from healthy

252   donors with the small-molecule XIAP antagonist embelin, which interacts with the same XIAP

253   BIR3 domain residues as caspase-9 [27], to mimic the in vivo EBV infection of XLP2 patients.

254   Embelin treatment significantly reduced the percentage of CD19+ B-cells at 7-day post-

255   infection, a timepoint at which most surviving B-cells are EBV-infected. However, embelin did

256   not significantly reduce CD56+ NK, CD4+ or CD8+ T-cell frequency in PBMC cultures (Figure

257   5A-B), suggesting an XIAP role in infected B-cell survival. To exclude the possibility that embelin

258   exhibits B cell-specific toxicity, we treated primary B cells with embelin prior to either EBV

259   infection or CD40L/IL21 stimulation. Consistent with our XIAP knockout results, embelin-treated

260   cells showed increased cell death only in EBV-infected B cells, while CD40L/IL21-stimulated

261   cells remained unaffected (Figure 5C). These findings suggest that embelin's effects closely

262   mimic those observed in XIAP-deficient cells, specifically targeting EBV-infected B cells without

263   general B cell toxicity.

264   Embelin reduction of EBV-infected B-cell numbers could be by effects on growth and/or survival.

265   To investigate this further, we stained the PBMC with CellTrace Violet and analyzed the CD19+

266   B cells with FACS dye-dilution analysis. Interestingly, we observed that markedly less

267   proliferation of EBV-infected CD19+ B-cells in embelin treated PBMC cultures, though analysis

268   was complicated by low numbers of live B-cells at this timepoint in embelin treated PBMCs

269   (Figure 5D). We therefore next analyzed embelin effects on CD19+ cell death, as judged by 7-

270   AAD uptake. Interestingly, embelin XIAP blockade increased EBV-infected B-cell cell death

271   when cultured with autologous PBMCs than when cultured alone (Figure 5E). These results

272   thus suggest that the presence of other immune cells further enhances the apoptosis of EBV-

273   infected cells.

274   We next sought to determine the factor that promotes the apoptosis of EBV infected cells.

275   Notably, multiple pro-inflammatory cytokine levels are elevated in XLP-2 patient serum in

276   particular IL-18, IL-6, interferon gamma (IFNγ) and tumor necrosis factor alpha (TNFα) [38]. EBV

277   infection also upregulates infected B-cell expression of multiple pro-inflammatory cytokines, and

278   IL-18, TNFα and IFNγ mRNAs are upregulated within the first week of EBV infection [33]. Since

279   pro-inflammatory cytokines can sensitize cells to apoptosis, we hypothesized that XIAP

280   deficiency and pro-inflammatory cytokines might exert synthetic effects that together potentiate

281   apoptosis of newly EBV-infected cells. To test this hypothesis, we treated EBV-infected purified

282   B-cells from three healthy donors with vehicle or embelin, together with vehicle, IFNγ, TNFα, IL-

283   5 or IL-18. Intriguingly, IFNγ and to a lesser extent TNFα treatment significantly increased

284   caspase 3/7 activity in embelin but not DMSO-treated cells (Figure 5F). Interestingly, IFNg

285   treatment also strongly suppressed outgrowth of embelin treated but not vehicle treated EBV-

286   infected B-cells over the first two weeks (Figure 5G). These findings indicate that XIAP inhibition

287   in newly EBV-infected cells renders the cells sensitive to inflammatory cytokines.

288   Collectively, our data is consistent with a model in which EBV triggers p53-mediated apoptotic

289   signaling, which results in activation of caspase 3 and 7. Existence of XIAP in the host cells can

290   inhibit this signaling, thus allowing for cell survival and B cell transformation. In patients with

291   XLP2, mutation of XIAP makes the cells sensitive to p53-mediated apoptotic signaling and

292   inflammatory cytokines, resulting in cell death of EBV infected cells, thus abolishing

293   lymphomagenesis (Figure 6).

Discussion

The absence of EBV-associated lymphoma is a striking feature of XLP2, which separates it from XLP1 and from nearly all other immunodeficiencies with defective cell mediated control of EBV-infected B-cells. Here, we used multidisciplinary approaches to characterize how XIAP perturbation by XLP2 mutation, CRISPR editing or small molecule inhibition alters EBV/B-cell interactions and early events in EBV-driven B-cell transformation. Multi-omic profiling highlighted that in the absence of XIAP, EBV upregulates caspase 3 and 7 activity in a p53 and BAX dependent manner over the first week of primary B-cell infection, limiting transforming B-cell outgrowth. Co-incubation with IFNγ or TNFα, which are found in XLP2 serum at elevated levels in particular in the setting of HLH, strongly further suppressed EBV immortalization of XIAP depleted B-cells.

XLP2 lymphocytes display increased susceptibility to extrinsic apoptosis triggered by CD95/FAS, TNFα or TNF related apoptosis-inducing ligand (TRAIL), and XLP2 T-cells also exhibit increased rates of activation-induced programmed cell death [18,39]. However, EBV can convert XLP2 B-cells with loss-of-function XIAP mutations into continuously growing, immortalized lymphoblastoid cell lines (LCLs) in culture [24], which are a key model for EBV-driven immunoblastic lymphomas of immunocompromised hosts. Our findings indicate that XIAP is not critical for growth or survival of infected cells that convert to lymphoblastoid physiology over the first weeks of infection. Furthermore, CRISPR XIAP KO does not significantly alter the growth or survival of established LCLs [24] and did not score in a human genome-wide CRISPR screen for LCL dependency factors [40]. Therefore, the question of why EBV+ lymphomas are not observed in XLP2 patients has remained open.

We now suggest that XIAP plays key roles in support of the earliest stages of EBV-mediated primary human B-cell transformation, particularly in the presence of elevated IFNγ and TNFα,

318   which are often found at elevated levels in XLP2 patients, who exhibit high rates of recurrent

319   splenomegaly and HLH [38]. Over the first three days post-infection, EBV remodels newly infected

320   B-cells, driving elevated levels of MYC expression, altering metabolism and quadrupling their

321   size. EBV then drives Burkitt-like B-cell hyperproliferation between days 3-7 post-infection

322   [30,31,41-43]. This aligns with our findings, where we observed extensive cell death in EBV-infected

323   *XIAP* knockout cells around day 4 post-infection. EBV then expresses increasing levels of the

324   oncogene LMP1, which mimics aspects of CD40 signaling, to convert B-cells to lymphoblastoid

325   B-cell physiology [44]. Key LMP1/NF-kB pathway targets include anti-apoptosis factors including

326   cIAP1, cIAP2, cFLIP and pro-survival BCL-2 family members [45,46]. LMP1 can also inhibit p53-

327   mediated apoptosis by inducing the deubiquitinase A20 [47]. However, EBV does not significantly

328   upregulate XIAP in transforming B-cells and p53 expression is sustained [30,33]. Therefore, our

329   results suggest that XIAP exerts key pro-survival roles likely in the Burkitt-like hyperproliferation

330   stage of EBV transformation, prior to the marked upregulation of anti-apoptotic factors by LMP1

331   and perhaps also prior to maximal inhibition of p53 signaling by EBNA3C [48,49]. Likewise,

332   following LMP1 upregulation, lymphoblastoid cells are not dependent on XIAP for growth or

333   survival.

334   What then triggers apoptosis signaling within the first week of EBV infection? EBV-driven B-

335   cell hyper-proliferation activates DNA damage responses (DDR), which signal through p53

336   [31,43,50,51]. Following the initial phase of rapid proliferation, by approximately day 7 post-EBV

337   infection, the proliferation rate slows. Our results suggest that such elevated p53 levels and

338   upregulation of p53 targets including NOXA and PUMA culminate in activation of BAX, which is

339   a three BH3-only (BCL-2 Homology domain) apoptosis effector. When expressed at elevated

340   levels and not sufficiently counteracted by pro-survival BCL2 family members, BAX undergoes

341   conformational changes, oligomerization and insertion into the mitochondrial outer membrane.

342   This enables egress of cytochrome c and other apoptogenic factors to activate executioner

343 caspase activity, including caspases 3 and 7 [34,35]. Our observations that the inhibition of p53 and

344 BAX can avert cell death in EBV-infected XIAP-deficient cells suggest that this apoptotic

345 pathway constitutes a pivotal mechanism of cell death during the initial stages of EBV infection.

346 Therefore, EBV driven B-cell hyperproliferation and DNA damage signaling creates a

347 dependency on XIAP prior to LMP1 upregulation, and this may serve to protect XLP2 B-cells

348 from undergoing full EBV immortalization, particularly in a hyper-inflammatory cytokine milieu.

349 This may also explain why we did not observe defects in XLP2 B-cell proliferation when

350 stimulated by CD40L/IL-21, which highly upregulates anti-apoptotic factors including cIAP1 and

351 2.

352 How does XIAP loss of function synergize with IFNγ and TNFα to antagonize EBV-mediated

353 B-cell transformation? P53 and IFNγ have an intricate cross-relationship, and it is plausible that

354 IFNγ treatment heightens sensitivity to p53-driven apoptosis signaling [52] in newly EBV-infected

355 B-cells. For instance, IFNγ can upregulate nuclear p53 expression and interaction with target

356 genes [53]. IFNγ can also block EBV-mediated B-cell transformation through incompletely

357 identified mechanisms [54]. TNFα may directly trigger apoptosis signaling in newly EBV-infected

358 B-cells that may necessitate XIAP activity for survival, as is observed in XIAP KO murine bone

359 marrow derived macrophages and in XIAP KO mice *in vivo* [39]. We note that EBV+

360 lymphoblastoid cells are also dependent on cFLIP to block TNFα-mediated apoptosis [40]. IFNγ

361 can also induce apoptosis, and this may be exacerbated by XIAP deficiency in infected B-cells

362 undergoing Burkitt-like hyperproliferation. Alternatively, IFNγ or TNFα may alter EBV oncogene

363 expression to interrupt EBV-driven B-cell immortalization over the first week of infection.

364 Identifying precise mechanisms by which IFNγ and TNFα each antagonize EBV-mediated B-cell

365 immortalization in the absence of XIAP will be an important objective.

366   A recent study identified that LCLs derived from XLP2 patients had modestly elevated lytic

367   gene expression [24]. However, we did not observe significantly elevated lytic gene expression in

368   our transcriptomic or proteomic profiling, suggesting that this phenomenon may be specific to

369   established LCLs and did not likely contribute to inhibition of EBV-infected B-cell outgrowth.

370   Similarly, the tumor suppressor cell adhesion molecule 1 (CADM1) was highly upregulated on

371   LCLs established from XLP2 B-cells. Consistent with this report, our proteomic profiling

372   identified CADM1 upregulation in XLP2 B-cells at 7 days post-infection (Table S2), suggesting

373   that this is an early phenomenon in EBV-infected XLP2 B-cells.

374   In summary, we identified a key role for XIAP in blockade of EBV-induced apoptosis signaling

375   within the first week of infection. Loss of XIAP function impaired proliferation and triggered

376   apoptosis of EBV+ B-cells, particularly at the Burkitt-like stage of hyperproliferation and prior to

377   full LMP1 upregulation and pro-survival signaling. This pro-apoptotic pathway was dependent

378   on p53- and BAX and was exacerbated by treatment IFNγ or TNFα, whose expression are

379   elevated with XLP2. Our results provide insights into the curious absence of EBV-driven

380   lymphoproliferative disease in XLP2 patients, despite heightened sensitivity to EBV.

381

382   **Acknowledgments**

387

388   **Author contributions**

389   Y.S. performed the experiments, data analysis, wrote the first draft and edited the manuscript

390   together with B.E.G; J.C. provided blood samples of XLP-2 patients and healthy controls; K.D.

391   performed mass spectrometry analysis; B.E.G. supervised the study. All authors read and

392   approved the final manuscript.

393

394   **Conflict-of-interest disclosure**

395   The authors declare no competing financial interests.

References

1.   Farrell PJ. Epstein–Barr Virus and Cancer. *Annual Review of Pathology: Mechanisms of Disease*. 2019;14(Volume 14, 2019):29-53.

2.   Münz C. Latency and lytic replication in Epstein–Barr virus-associated oncogenesis. *Nature Reviews Microbiology*. 2019;17(11):691-700.

3.   Cohen JI, Mocarski Es Fau - Raab-Traub N, Raab-Traub N Fau - Corey L, Corey L Fau - Nabel GJ, Nabel GJ. The need and challenges for development of an Epstein-Barr virus vaccine. (1873-2518 (Electronic)).

4.   Heslop HE. How I treat EBV lymphoproliferation. *Blood*. 2009;114(19):4002-4008.

5.   Tangye SG, Latour S. Primary immunodeficiencies reveal the molecular requirements for effective host defense against EBV infection. *Blood*. 2020;135(9):644-655.

6.   Cohen JI. Primary Immunodeficiencies Associated with EBV Disease. In: Münz C, ed. Epstein Barr Virus Volume 1: One Herpes Virus: Many Diseases. Cham: Springer International Publishing; 2015:241-265.

7.   Rickinson AB, Long HM, Palendira U, Münz C, Hislop AD. Cellular immune controls over Epstein-Barr virus infection: new lessons from the clinic and the laboratory. (1471-4981 (Electronic)).

8.   Parvaneh N, Filipovich AH, Borkhardt A. Primary immunodeficiencies predisposed to Epstein-Barr virus-driven haematological diseases. *British Journal of Haematology*. 2013;162(5):573-586.

9.   Chiu Y-F, Ponlachantra K, Sugden B. How Epstein Barr Virus Causes Lymphomas. Viruses. Vol. 16; 2024.

10.   Shannon-Lowe C, Rickinson AB, Bell AI. Epstein–Barr virus-associated lymphomas. *Philosophical Transactions of the Royal Society B: Biological Sciences*. 2017;372(1732):20160271.

11.   Taylor GS, Long HM, Brooks JM, Rickinson AB, Hislop AD. The Immunology of Epstein-Barr Virus–Induced Disease. *Annual Review of Immunology*. 2015;33(1):787-821.

12.   Meyer L, Hines M, Zhang K, Nichols KE. X-Linked Lymphoproliferative Disease. BTI - GeneReviews(®).

13.   Schmid JP, Canioni D, Moshous D, et al. Clinical similarities and differences of patients with X-linked lymphoproliferative syndrome type 1 (XLP-1/SAP deficiency) versus type 2 (XLP-2/XIAP deficiency). *Blood*. 2011;117(5):1522-1529.

14.   Henter J-I, Horne A, Aricó M, et al. HLH-2004: Diagnostic and therapeutic guidelines for hemophagocytic lymphohistiocytosis. *Pediatric Blood & Cancer*. 2007;48(2):124-131.

15.   Coffey AJ, Brooksbank RA, Brandau O, et al. Host response to EBV infection in X-linked lymphoproliferative disease results from mutations in an SH2-domain encoding gene. *Nature Genetics*. 1998;20(2):129-135.

16.   Sayos J, Wu C, Morra M, et al. The X-linked lymphoproliferative-disease gene product SAP regulates signals induced through the co-receptor SLAM. *Nature*. 1998;395(6701):462-469.

17.   Hanifeh M, Ataei F. XIAP as a multifaceted molecule in Cellular Signaling. *Apoptosis*. 2022;27(7):441-453.

18.   Rigaud S, Fondanèche M-C, Lambert N, et al. XIAP deficiency in humans causes an X-linked lymphoproliferative syndrome. *Nature*. 2006;444(7115):110-114.

19.   Huang Y, Park YC, Rich RL, Segal D, Myszka DG, Wu H. Structural Basis of Caspase Inhibition by XIAP: Differential Roles of the Linker versus the BIR Domain. *Cell*. 2001;104(5):781-790.

20.   Galbán S, Duckett CS. XIAP as a ubiquitin ligase in cellular signaling. *Cell Death & Differentiation*. 2010;17(1):54-60.

21.   Filipovich AH, Zhang K, Snow AL, Marsh RA. X-linked lymphoproliferative syndromes: brothers or distant cousins? *Blood*. 2010;116(18):3398-3408.

442 22. Tangye SG. XLP: Clinical Features and Molecular Etiology due to Mutations in SH2D1A Encoding
443 SAP. *Journal of Clinical Immunology*. 2014;34(7):772-779.
444 23. Latour S, Aguilar C. XIAP deficiency syndrome in humans. *Seminars in Cell & Developmental*
445 *Biology*. 2015;39:115-123.
446 24. Engelmann C, Schuhmachers P, Zdimerova H, et al. Epstein Barr virus-mediated transformation of
447 B cells from XIAP-deficient patients leads to increased expression of the tumor suppressor CADM1. *Cell*
448 *Death & Disease*. 2022;13(10):892.
449 25. Hunte R, Alonso P, Thomas R, et al. CADM1 is essential for KSHV-encoded vGPCR-and vFLIP-
450 mediated chronic NF-κB activation. *PLOS Pathogens*. 2018;14(4):e1006968.
451 26. Good KL, Bryant VL, Tangye SG. Kinetics of Human B Cell Behavior and Amplification of
452 Proliferative Responses following Stimulation with IL-211. *The Journal of Immunology*. 2006;177(8):5236-
453 5247.
454 27. Nikolovska-Coleska Z, Xu L, Hu Z, et al. Discovery of Embelin as a Cell-Permeable, Small-
455 Molecular Weight Inhibitor of XIAP through Structure-Based Computational Screening of a Traditional
456 Herbal Medicine Three-Dimensional Structure Database. *Journal of Medicinal Chemistry*.
457 2004;47(10):2430-2440.
458 28. Chou J, Platt CD, Habiballah S, et al. Mechanisms underlying genetic susceptibility to multisystem
459 inflammatory syndrome in children (MIS-C). *Journal of Allergy and Clinical Immunology*.
460 2021;148(3):732-738.e731.
461 29. Philipp J, Vucic D. Regulation of Cell Death and Immunity by XIAP. *Cold Spring Harbor*
462 *perspectives in biology*. 2020;12(8):a036426.
463 30. Wang LW, Shen H, Nobre L, et al. Epstein-Barr-Virus-Induced One-Carbon Metabolism Drives B
464 Cell Transformation. *Cell Metabolism*. 2019;30(3):539-555.e511.
465 31. Nikitin PA, Yan CM, Forte E, et al. An ATM/Chk2-Mediated DNA Damage-Responsive Signaling
466 Pathway Suppresses Epstein-Barr Virus Transformation of Primary Human B Cells. *Cell Host & Microbe*.
467 2010;8(6):510-522.
468 32. Pich D, Mrozek-Gorska P, Bouvet M, et al. First Days in the Life of Naive Human B Lymphocytes
469 Infected with Epstein-Barr Virus. *mBio*. 2019;10(5):10.1128/mbio.01723-01719.
470 33. Wang C, Li D, Zhang L, et al. RNA Sequencing Analyses of Gene Expression during Epstein-Barr
471 Virus Infection of Primary B Lymphocytes. *Journal of Virology*. 2019;93(13):10.1128/jvi.00226-00219.
472 34. Lomonosova E, Chinnadurai G. BH3-only proteins in apoptosis and beyond: an overview.
473 *Oncogene*. 2008;27(1):S2-S19.
474 35. Aubrey BJ, Kelly GL, Janic A, Herold MJ, Strasser A. How does p53 induce apoptosis and how
475 does this relate to p53-mediated tumour suppression? *Cell Death & Differentiation*. 2018;25(1):104-113.
476 36. Garner TP, Amgalan D, Reyna DE, Li S, Kitsis RN, Gavathiotis E. Small-molecule allosteric inhibitors
477 of BAX. *Nature Chemical Biology*. 2019;15(4):322-330.
478 37. Komarov PG, Komarova EA, Kondratov RV, et al. A Chemical Inhibitor of p53 That Protects Mice
479 from the Side Effects of Cancer Therapy. *Science*. 1999;285(5434):1733-1737.
480 38. Wada T, Kanegane H, Ohta K, et al. Sustained elevation of serum interleukin-18 and its
481 association with hemophagocytic lymphohistiocytosis in XIAP deficiency. *Cytokine*. 2014;65(1):74-78.
482 39. Witt A, Goncharov T, Lee YM, et al. XIAP deletion sensitizes mice to TNF-induced and RIP1-
483 mediated death. *Cell Death Dis*. 2023;14(4):262.
484 40. Ma Y, Walsh MJ, Bernhardt K, et al. CRISPR/Cas9 Screens Reveal Epstein-Barr Virus-Transformed
485 B Cell Host Dependency Factors. *Cell Host Microbe*. 2017;21(5):580-591 e587.
486 41. Wang LW, Wang Z, Ersing I, et al. Epstein-Barr virus subverts mevalonate and fatty acid pathways
487 to promote infected B-cell proliferation and survival. *PLoS Pathog*. 2019;15(9):e1008030.
488 42. Mrozek-Gorska P, Buschle A, Pich D, et al. Epstein-Barr virus reprograms human B lymphocytes
489 immediately in the prelatent phase of infection. *Proc Natl Acad Sci U S A*. 2019;116(32):16046-16055.

490   43.   McFadden K, Hafez AY, Kishton R, et al. Metabolic stress is a barrier to Epstein-Barr virus-
491   mediated B-cell immortalization. *Proc Natl Acad Sci U S A*. 2016;113(6):E782-790.
492   44.   Price AM, Tourigny JP, Forte E, Salinas RE, Dave SS, Luftig MA. Analysis of Epstein-Barr virus-
493   regulated host gene expression changes through primary B-cell outgrowth reveals delayed kinetics of
494   latent membrane protein 1-mediated NF-kappaB activation. *J Virol*. 2012;86(20):11096-11106.
495   45.   Price AM, Dai J, Bazot Q, et al. Epstein-Barr virus ensures B cell survival by uniquely modulating
496   apoptosis at early and late times after infection. *Elife*. 2017;6.
497   46.   Mitra B, Beri NR, Guo R, Burton EM, Murray-Nerger LA, Gewurz BE. Characterization of target
498   gene regulation by the two Epstein-Barr virus oncogene LMP1 domains essential for B-cell
499   transformation. *mBio*. 2023;14(6):e0233823.
500   47.   Husaini R, Ahmad M, Soo-Beng Khoo A. Epstein-Barr virus Latent Membrane Protein LMP1
501   reduces p53 protein levels independent of the PI3K-Akt pathway. *BMC Res Notes*. 2011;4:551.
502   48.   Saha A, Murakami M, Kumar P, Bajaj B, Sims K, Robertson ES. Epstein-Barr virus nuclear antigen
503   3C augments Mdm2-mediated p53 ubiquitination and degradation by deubiquitinating Mdm2. *J Virol*.
504   2009;83(9):4652-4669.
505   49.   Yi F, Saha A, Murakami M, et al. Epstein-Barr virus nuclear antigen 3C targets p53 and modulates
506   its transcriptional and apoptotic activities. *Virology*. 2009;388(2):236-247.
507   50.   Nikitin PA, Price AM, McFadden K, Yan CM, Luftig MA. Mitogen-induced B-cell proliferation
508   activates Chk2-dependent G1/S cell cycle arrest. *PLoS One*. 2014;9(1):e87299.
509   51.   Koganti S, Hui-Yuen J, McAllister S, et al. STAT3 interrupts ATR-Chk1 signaling to allow oncovirus-
510   mediated cell proliferation. *Proc Natl Acad Sci U S A*. 2014;111(13):4946-4951.
511   52.   Ossina NK, Cannas A, Powers VC, et al. Interferon-gamma modulates a p53-independent
512   apoptotic pathway and apoptosis-related gene expression. *J Biol Chem*. 1997;272(26):16351-16357.
513   53.   Contreras AU, Mebratu Y, Delgado M, et al. Deacetylation of p53 induces autophagy by
514   suppressing Bmf expression. *J Cell Biol*. 2013;201(3):427-437.
515   54.   Lunemann A, Vanoaica LD, Azzi T, Nadal D, Munz C. A distinct subpopulation of human NK cells
516   restricts B cell transformation by EBV. *J Immunol*. 2013;191(10):4989-4995.
517

Figure Legends

Figure 1. XIAP inactivation impairs the outgrowth of newly EBV infected primary B-cells.

(A) Workflow for electroporation and EBV infection of primary human B-cells. B-cells purified

from peripheral blood mononuclear cells (PBMC) were transduced with Cas9 ribonucleoprotein

(RNP) complexes containing *XIAP* targeting or non-targeting control single guide RNA (sgRNA).

1 hour post electroporation, cells were infected with EBV or stimulated by CD40 ligand (CD40L)

(50 ng/ml) and IL-21 (50 ng/ml).

(B) Immunoblot analysis of whole cell lysates (WCL) from primary B-cells on day 3 post

electroporation with Cas9 control (ctrl) or XIAP sgRNA containing RNPs.

(C) XIAP editing does not alter EBV infection efficiency. FACS analysis of control versus XIAP

edited B-cells at Day 2 post-infection by recombinant EBV that expresses a green fluorescence

protein (GFP) marker. Mean + standard deviation (SD) GFP+ cell percentages from n=3

replicates are shown on the right.

(D) Growth curve analysis of primary human B-cells transfected with the indicated sgRNA-

containing Cas9 RNPs and treated with CD40L and IL-21 or infected with EBV. CD40L/IL-21

were replenished every 3 days. Mean ± SD fold change live cell numbers from n = 3 biological

replicates, relative to Day 0 values, are shown.

(E) Immunoblot analysis of WCL from primary B-cells with control or XIAP sgRNA-containing

RNP on the indicated days post-EBV infection.

(F) Growth curve analysis of primary B-cells treated with DMSO or the XIAP inhibitor embelin (5

µM) together with EBV infection (left) or CD40L/IL-21 treatment (right). Embelin, CD40L and IL-

21 were replenished every 3 days. Mean ± SD fold change live cell numbers from n=3

replicates, relative to Day 0 values, are shown.

(G) Immunoblot and growth curve analysis of Cas9+ GM12878 LCLs expressing the indicated

control or independent *XIAP* targeting sgRNAs. Mean ± SD fold change live cell numbers from

n=3 replicates, relative to Day 0 values, are shown.

544   (H) Growth curves analysis of GM12878 LCLs treated with DMSO or embelin (5 µM), which

545   were replenished every 3 days. Mean ± SD fold change live cell numbers from n=3 replicates,

546   relative to Day 0 values, are shown.

547   (I) Growth curve analysis of primary human B-cells infected by EBV at Day 0 and then treated

548   with embelin (5 µM) over the indicated times. Embelin was replenished every 3 days. Mean ±

549   SD fold change live cell numbers from n=3 replicates, relative to Day 0 values, are shown.

550   Statistical significance was assessed by comparing each indicated groups with DMSO control

551   groups.

552   Statistical significance was assessed by two-tailed unpaired Student's t test (C, D, F, H, I) or

553   one-way ANOVA followed by Tukey's multiple comparisons test (G). Blots are representative of

554   n=3 replicates. **p<0.01, ***p<0.001, ****p<0.0001, ns, not significant.

555

556   **Figure 2. XLP2 patient B-cells demonstrate impaired EBV but not CD40L/IL-21 driven**

557   **outgrowth at early timepoints.**

558   (A) Schematic diagram highlighting the *XIAP* mutation shared by XLP2 Patients #1 and #2.

559   (B) Growth curve analysis of primary B-cells from XLP2 patients or from controls that were

560   infected with EBV. Mean ± SD fold change live cell numbers from n=3 replicates, relative to Day

561   0 values, are shown. The annotations represent the results of statistical comparisons between

562   XLP2 samples and Control #1.

563   (C) Growth curve analysis of primary B-cells from XLP2 patients or controls treated with CD40L

564   and IL-21, which was replenished every 3 days. Mean ± SD fold change live cell numbers from

565   n=3 replicates, relative to Day 0 values, are shown. The annotations represent the results of

566   statistical comparisons between XLP2 samples and Control #1.

567   (D) Growth curves of lymphoblastoid cells established from B cells from either two XLP2

568   patients or three controls. Mean ± SD fold change live cell numbers from n=3 replicates, relative

569   to Day 0 values, are shown. The annotations represent the results of statistical comparisons

570   between XLP2 samples and Control #1.

571   (E) EBV B-cell transformation assay workflow. CD19+ B-cells purified from PBMCs were plated

572   and infected with serial dilutions of the Akata EBV strain, using a range of 0 – 100 EBV

573   transforming units/well. Wells with B-cell outgrowth were scored 4 weeks later. Outgrowth wells

574   on one of the three replicate plates were displayed.

575   (F) EBV transformation assays of primary human B-cells from XLP2 patient or healthy controls,

576   as in (E). Shown are the mean ± SD percentages of wells with B-cell outgrowth from n=3

577   replicates.

578   Statistical significance was assessed by one-way ANOVA followed by Tukey's multiple

579   comparisons test (B-D, F). *p<0.05, **p<0.01, ***p<0.001, ****, p<0.0001, ns, non-significant.

580

581   **Figure 3. EBV but not CD40L/IL-21 triggers apoptosis within the first week of XLP2 B-cell**

582   **infection.**

583   (A) FACS analysis of control versus XIAP edited primary human B-cells at Day 4 post-EBV

584   infection or CD40L/IL-21 stimulation. Shown are representative FACS plots from n=3 replicates

585   of cells stained with CFSE prior to EBV infection or CD40L/IL-21 treatment. Live cells were

586   gated by absence of 7-AAD vital dye uptake.

587   (B) Mean + SD Percentages of cells with the indicated number of mitoses from n=3 replicates

588   as in (A) of EBV infection versus CD40L/IL-21 stimulation.

589   (C) Mean + SD % 7AAD+ cells from n=3 replicates of control or XIAP edited primary B-cells on

590   Day 4 post-EBV infection or CD40L/IL21 treatment.

591   (D) Mean + SD caspase 3/7 activity from n=3 replicates of control or XIAP edited primary B-cells

592   on day 4 post-EBV infection or CD40L/IL-21 treatment.

593   (E) Mean + SD caspase 3/7 activity from n=3 replicates of control or XLP2 primary B-cells on

594   day 4 post-EBV infection or CD40L/IL-21 treatment.

24

595   (F) Mean + SD caspase 3/7 activity from n=3 replicates of control or XIAP edited primary B-cells

596   incubated with DMSO vehicle or the pan-caspase inhibitor zVAD-fmk (20 μM) on day 4 post-

597   EBV infection or CD40L/IL-21 treatment.

598   (G) Mean + SD % 7AAD+ cells from n=3 replicates of control or XIAP edited primary B-cells on

599   Day 4 post-EBV infection or CD40L/IL21 treatment.

600   (H) Growth curve analysis of control versus *XIAP* edited primary B-cells infected with EBV on

601   Day 0 and cultured with DMSO vehicle or zVAD-Fmk (20 μM). Mean ± SD fold change live cell

602   numbers, relative to uninfected values, are shown. DMSO or zVAD-Fmk were replenished every

603   3 days.

604   Statistical significance was assessed by two-tailed unpaired Student's t test (B-D, H) or one (E)

605   or two-way (F and G) ANOVA followed by Tukey's multiple comparisons test. In A-G, CD40L and

606   IL21 were replenished on Day 3. **p<0.01, ***p<0.001, ****p<0.0001. ns, not significant.

607

608   **Figure 4. EBV but not CD40L/IL-21 activates p53- and BAX-dependent apoptosis in newly**

609   **infected XIAP deficient B-cells.**

610   (A) Heatmap of RNAseq analysis of primary B-cells from XLP2 patient or controls on Day 7-post

611   EBV infection or CD40L/IL-21 treatment. Z-scores of normalized reads of the indicated mRNAs

612   from n=3 replicates are shown. Columns show data from two XLP2 patients or three controls.

613   (B) Multiplexed tandem mass tag proteomic analysis of primary B-cells from XLP2 patients or

614   healthy controls on Day 7 post-EBV infection or CD40L/IL-21 treatment. Unstimulated cells were

615   harvested on Day 0. Z-scores of relative protein abundances of the indicated mRNAs from n=3

616   replicates are shown. Columns show data from two XLP2 patients or three controls.

617   (C) Mean + standard deviation (SD) TP53 and BAX mRNA expression from n=3 replicates of

618   RNAseq analysis of primary human B-cells on the indicated days post EBV infection [33].

25

619   (D) Schematic diagram illustrating p53 that p53 target genes PUMA and NOXA can each

620   upregulate BAX, which in turn induces the intrinsic apoptosis pathway. Red stars denote

621   upregulation at Day 7 post-EBV infection relative to CD40L/IL-21 levels.

622   (E) Mean + SD caspase 3/7 activity from n=3 replicates of primary B-cells expressing control or

623   XIAP targeting sgRNAs and treated with BAI1 (5 µM) on day 4 post EBV infection. BAI1 was

624   added from Day 0 onwards, replenished every 3 days.

625   (F) Growth curve analysis of control versus *XIAP* edited primary B-cells and cultured with

626   DMSO, zVAD-Fmk (20 µM) or BAI1 (5 µM) from Day 0 onwards. Mean ± SD fold change live

627   cell numbers, relative to uninfected values, are shown. DMSO, BAI and zVAD-Fmk were

628   replenished every 3 days.

629   (G) Mean + SD caspase 3/7 activity from n=3 replicates of control versus *XIAP* edited primary

630   B-cells cultured with DMSO or pifithrin-α at 5 or 20 μM on Day 4 post-infection.

631   Statistical significance was assessed by two-tailed unpaired Student's t test (F) or two-way

632   ANOVA followed by Tukey's multiple comparisons test (E and G). *p<0.05, ***p<0.001,

633   ****p<0.0001.

634

635   **Figure 5. Embelin XIAP inhibition perturbs EBV-mediated primary B-cell outgrowth and**

636   **sensitizes newly-infected cells to IFNγ-triggered apoptosis.**

637   (A) FACS analysis of CD4+ or CD8+ T cell, CD56$^+$ NK cell and CD19+ B-cell subsets from

638   PBMCs of a control donor, infected with EBV and treated with DMSO or embelin (5 µM) on Day

639   7 post-EBV infection. DMSO and embelin were added starting from Day 0 and replenished

640   every 3 days.

641   (B) Mean + SD percentages of CD4+ or CD8+ T cell, CD56$^+$ NK cell and CD19+ B-cells from (A)

642   are shown.

643　(C) Mean + SD % 7AAD+ cells from n=3 replicates of DMSO or embelin treated primary B-cells

644　on Day 4 post-EBV infection or CD40L/IL21 treatment. DMSO and embelin were added starting

645　from Day 0 and replenished every 3 days.

646　(D) FACS analysis of CD19+ B-cells CellTrace Violet (CTV) dye dilution, whose abundance is

647　reduced by half with each mitosis, from PBMCs treated with DMSO (control) or embelin (5 µM)

648　on Day 7 post-EBV infection. The whole PBMC cell cultures were stained with CTV and infected

649　with EBV and treated with DMSO or embelin (5 µM) as in (A). Cells were stained with anti-CD19

650　antibodies on day 7 and CTV on CD19+ B cell was analyzed. DMSO and embelin were added

651　starting from Day 0 and replenished every 3 days.

652　(E) Mean + SD percentages of 7AAD+ cells of primary human B-cells from controls, cultured

653　alone or co-cultured with autologous PBMC in the presence of DMSO versus embelin (5 µM) for

654　4 days. B-cells were stained with CFSE prior to PBMC co-culture, which served as a cell trace

655　marker to allow their FACS gating within mixed PBMC cultures.

656　(F) Mean + SD caspase 3/7 activity from n=3 replicates of EBV-infected DMSO or embelin

657　treated cells that were co-cultured with PBS vehicle, IFNg (50 ng/mL), TNFa (50 ng/mL), IL-6

658　(50 ng/mL) or IL-18 (50 ng/mL) on Day 4 post-infection.

659　(G) Growth curve analysis of control primary human B-cells infected by EBV and treated with

660　DMSO or embelin (5 µM) together with IFNγ, TNFα, IL-6 or IL-18 as indicated. Shown are mean

661　± SD fold change live cell numbers from n=3 replicates. Statistical significance was assessed by

662　comparing each cytokine treated group with PBS control group.

663　Statistical significance was assessed by two-tailed unpaired Student's t test (B, C, G) or two-

664　way ANOVA followed by Tukey's multiple comparisons test (E and F). In all experiments, DMSO,

665　Embelin and cytokines were refreshed every 3 days. *p<0.05, **p<0.01, ***p<0.001,

666　****p<0.0001. ns, not significant.

667

668　**Figure 6. Schematic model of key anti-apoptotic XIAP role in newly EBV-infected B-cells.**

669   EBV drives rapid proliferation of newly infected B-cells, which triggers DNA damage,

670   upregulation of p53 and of downstream NOXA, PUMA and BAX. XIAP blocks caspase activity

671   and apoptosis in most settings, including with XLP1, enabling newly EBV-infected B-cells to

672   undergo transformation and in XLP1 to cause high rates of lymphomas. Lymphomas are not

673   observed in XLP2 patients, where the absence of XIAP enables caspase 3/7 activation and

674   apoptosis induction over the first week of EBV infection, which is exacerbated by the

675   inflammatory cytokine milieu, in particular IFNγ, restraining lymphomagenesis.

Figure 1

Figure 1. XIAP inactivation impairs the outgrowth of newly EBV infected primary B-cells.

(A) Workflow for electroporation and EBV infection of primary human B-cells. B-cells purified from peripheral blood mononuclear cells (PBMC) were transduced with Cas9 ribonucleoprotein (RNP) complexes containing XIAP targeting or non-targeting control single guide RNA (sgRNA). 1 hour post electroporation, cells were infected with EBV or stimulated by CD40 ligand (CD40L) (50 ng/ml) and IL-21 (50 ng/ml).

(B) Immunoblot analysis of whole cell lysates (WCL) from primary B-cells on day 3 post electroporation with Cas9 control (ctrl) or XIAP sgRNA containing RNPs.

(C) XIAP editing does not alter EBV infection efficiency. FACS analysis of control versus XIAP edited B-cells at Day 2 post-infection by recombinant EBV that expresses a green fluorescence protein (GFP) marker. Mean + standard deviation (SD) GFP+ cell percentages from n=3 replicates are shown on the right.

(D) Growth curve analysis of primary human B-cells transfected with the indicated sgRNA-containing Cas9 RNPs and treated with CD40L and IL-21 or infected with EBV. CD40L/IL-21 were replenished every 3 days. Mean ± SD fold change live cell numbers from n = 3 biological replicates, relative to Day 0 values, are shown.

(E) Immunoblot analysis of WCL from primary B-cells with control or XIAP sgRNA-containing RNP on the indicated days post-EBV infection.

(F) Growth curve analysis of primary B-cells treated with DMSO or the XIAP inhibitor embelin (5 µM) together with EBV infection (left) or CD40L/IL-21 treatment (right). Embelin, CD40L and IL-21 were replenished every 3 days. Mean ± SD fold change live cell numbers from n=3 replicates, relative to Day 0 values, are shown.
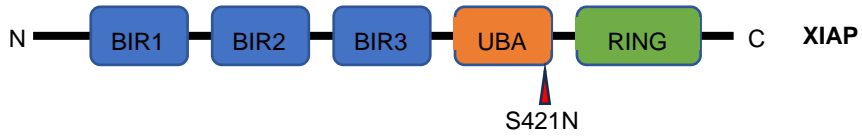
(G) Immunoblot and growth curve analysis of Cas9+ GM12878 LCLs expressing the indicated control or independent XIAP targeting sgRNAs. Mean ± SD fold change live cell numbers from n=3 replicates, relative to Day 0 values, are shown.

(H) Growth curves analysis of GM12878 LCLs treated with DMSO or embelin (5 µM), which were replenished every 3 days. Mean ± SD fold change live cell numbers from n=3 replicates, relative to Day 0 values, are shown.
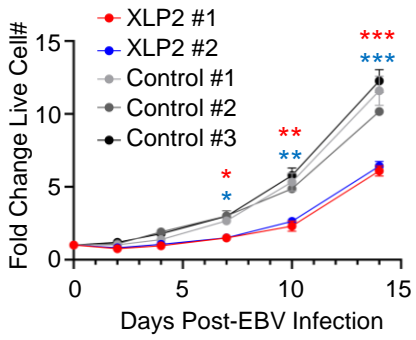
(I) Growth curve analysis of primary human B-cells infected by EBV at Day 0 and then treated with embelin (5 µM) over the indicated times. Embelin was replenished every 3 days. Mean ± SD fold change live cell numbers from n=3 replicates, relative to Day 0 values, are shown. Statistical significance was assessed by comparing each indicated groups with DMSO control groups.

Statistical significance was assessed by two-tailed unpaired Student's t test (C, D, F, H, I) or one-way ANOVA followed by Tukey's multiple comparisons test (G). Blots are representative of n=3 replicates. **p<0.01, ***p<0.001, ****p<0.0001, ns, not significant.
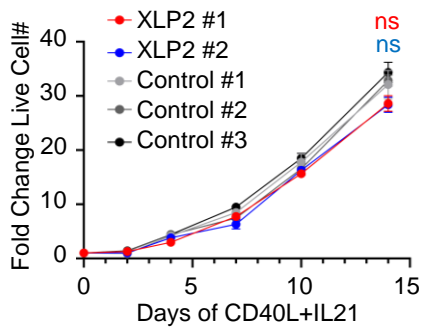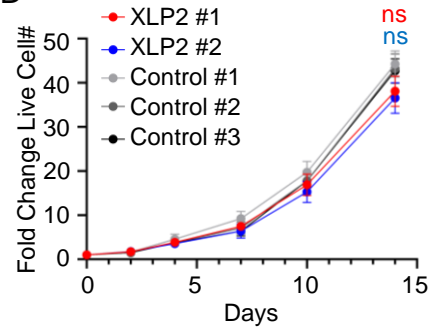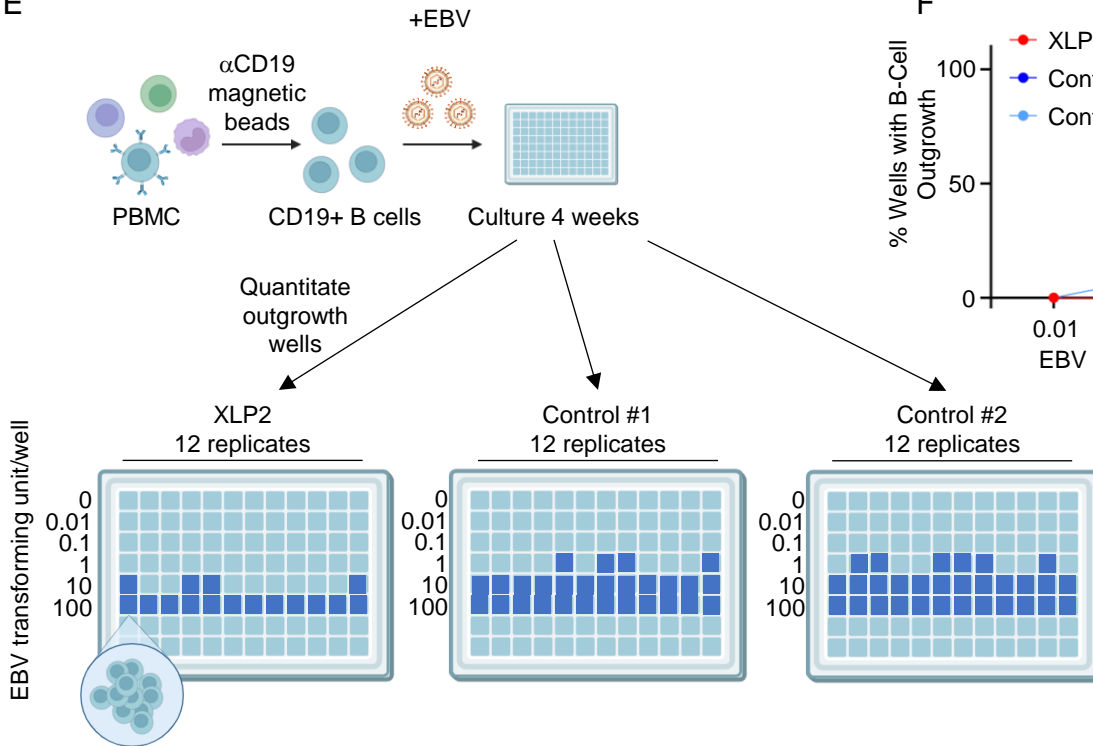
Figure 2

A

BIR1 · BIR2 · BIR3 · UBA · RING · XIAP

N · C

S421N

B

- XLP2 #1
- XLP2 #2
- Control #1
- Control #2
- Control #3

Fold Change Live Cell#

Days Post-EBV Infection

***
***
**
**
*
*

C

- XLP2 #1
- XLP2 #2
- Control #1
- Control #2
- Control #3

ns
ns

Fold Change Live Cell#

Days of CD40L+IL21

D

- XLP2 #1
- XLP2 #2
- Control #1
- Control #2
- Control #3

ns
ns

Fold Change Live Cell#

Days

E

+EBV

αCD19 magnetic beads

PBMC → CD19+ B cells → Culture 4 weeks

Quantitate outgrowth wells

XLP2
12 replicates

Control #1
12 replicates

Control #2
12 replicates

EBV transforming unit/well

0
0.01
0.1
1
10
100

F

- XLP2
- Control #1
- Control #2

% Wells with B-Cell Outgrowth
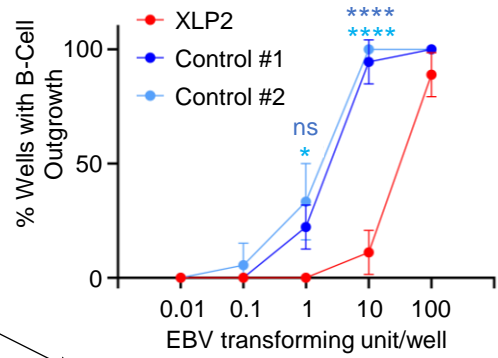
EBV transforming unit/well

****
****
ns
*

Figure 2. XLP2 patient B-cells demonstrate impaired EBV but not CD40L/IL-21 driven outgrowth at early timepoints.

(A) Schematic diagram highlighting the XIAP mutation shared by XLP2 Patients #1 and #2.

(B) Growth curve analysis of primary B-cells from XLP2 patients or from controls that were infected with EBV. Mean ± SD fold change live cell numbers from n=3 replicates, relative to Day 0 values, are shown. The annotations represent the results of statistical comparisons between XLP2 samples and Control #1.

(C) Growth curve analysis of primary B-cells from XLP2 patients or controls treated with CD40L and IL-21, which was replenished every 3 days. Mean ± SD fold change live cell numbers from n=3 replicates, relative to Day 0 values, are shown. The annotations represent the results of statistical comparisons between XLP2 samples and Control #1.

(D) Growth curves of lymphoblastoid cells established from B cells from either two XLP2 patients or three controls. Mean ± SD fold change live cell numbers from n=3 replicates, relative to Day 0 values, are shown. The annotations represent the results of statistical comparisons between XLP2 samples and Control #1.

(E) EBV B-cell transformation assay workflow. CD19+ B-cells purified from PBMCs were plated and infected with serial dilutions of the Akata EBV strain, using a range of 0 – 100 EBV transforming units/well. Wells with B-cell outgrowth were scored 4 weeks later. Outgrowth wells on one of the three replicate plates were displayed.

(F) EBV transformation assays of primary human B-cells from XLP2 patient or healthy controls, as in (E). Shown are the mean ± SD percentages of wells with B-cell outgrowth from n=3 replicates.

Statistical significance was assessed by one-way ANOVA followed by Tukey's multiple comparisons test (B-D, F). *p<0.05, **p<0.01, ***p<0.001, ****, p<0.0001, ns, non-significant.
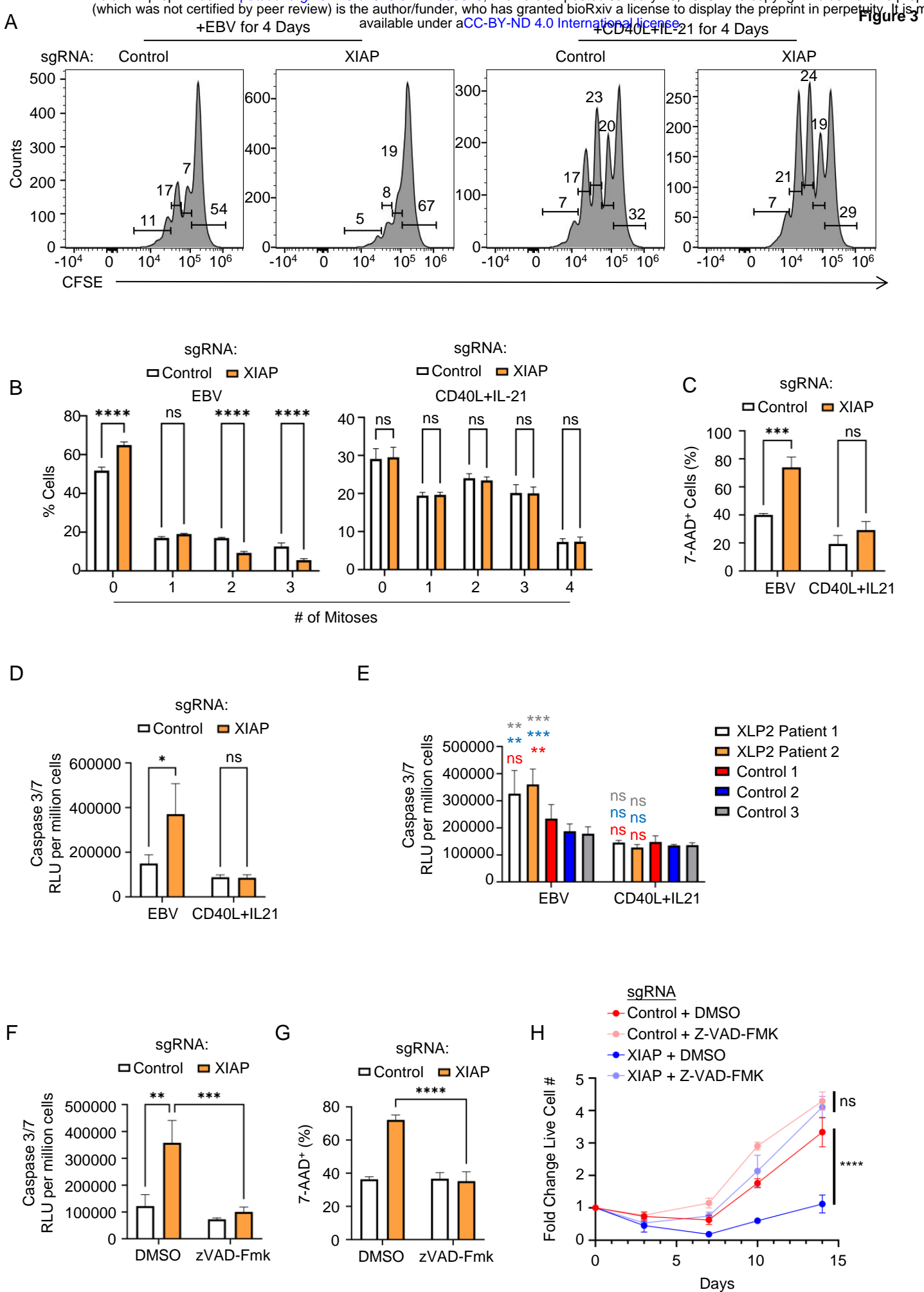
Figure 3

Figure 3. EBV but not CD40L/IL-21 triggers apoptosis within the first week of XLP2 B-cell infection.

(A) FACS analysis of control versus XIAP edited primary human B-cells at Day 4 post-EBV infection or CD40L/IL-21 stimulation. Shown are representative FACS plots from n=3 replicates of cells stained with CFSE prior to EBV infection or CD40L/IL-21 treatment. Live cells were gated by absence of 7-AAD vital dye uptake.

(B) Mean + SD Percentages of cells with the indicated number of mitoses from n=3 replicates as in (A) of EBV infection versus CD40L/IL-21 stimulation.

(C) Mean + SD % 7AAD+ cells from n=3 replicates of control or XIAP edited primary B-cells on Day 4 post-EBV infection or CD40L/IL21 treatment.

(D) Mean + SD caspase 3/7 activity from n=3 replicates of control or XIAP edited primary B-cells on day 4 post-EBV infection or CD40L/IL-21 treatment.

(E) Mean + SD caspase 3/7 activity from n=3 replicates of control or XLP2 primary B-cells on day 4 post-EBV infection or CD40L/IL-21 treatment.

(F) Mean + SD caspase 3/7 activity from n=3 replicates of control or XIAP edited primary B-cells incubated with DMSO vehicle or the pan-caspase inhibitor zVAD-fmk (20 µM) on day 4 post-EBV infection or CD40L/IL-21 treatment.

(G) Mean + SD % 7AAD+ cells from n=3 replicates of control or XIAP edited primary B-cells on Day 4 post-EBV infection or CD40L/IL21 treatment.

(H) Growth curve analysis of control versus XIAP edited primary B-cells infected with EBV on Day 0 and cultured with DMSO vehicle or zVAD-Fmk (20 µM). Mean ± SD fold change live cell numbers, relative to uninfected values, are shown. DMSO or zVAD-Fmk were replenished every 3 days.

Statistical significance was assessed by two-tailed unpaired Student's t test (B-D, H) or one (E) or two-way (F and G) ANOVA followed by Tukey's multiple comparisons test. In A-G, CD40L and IL21 were replenished on Day 3. **p<0.01, ***p<0.001, ****p<0.0001. ns, not significant.

Figure 4

A

RNAseq
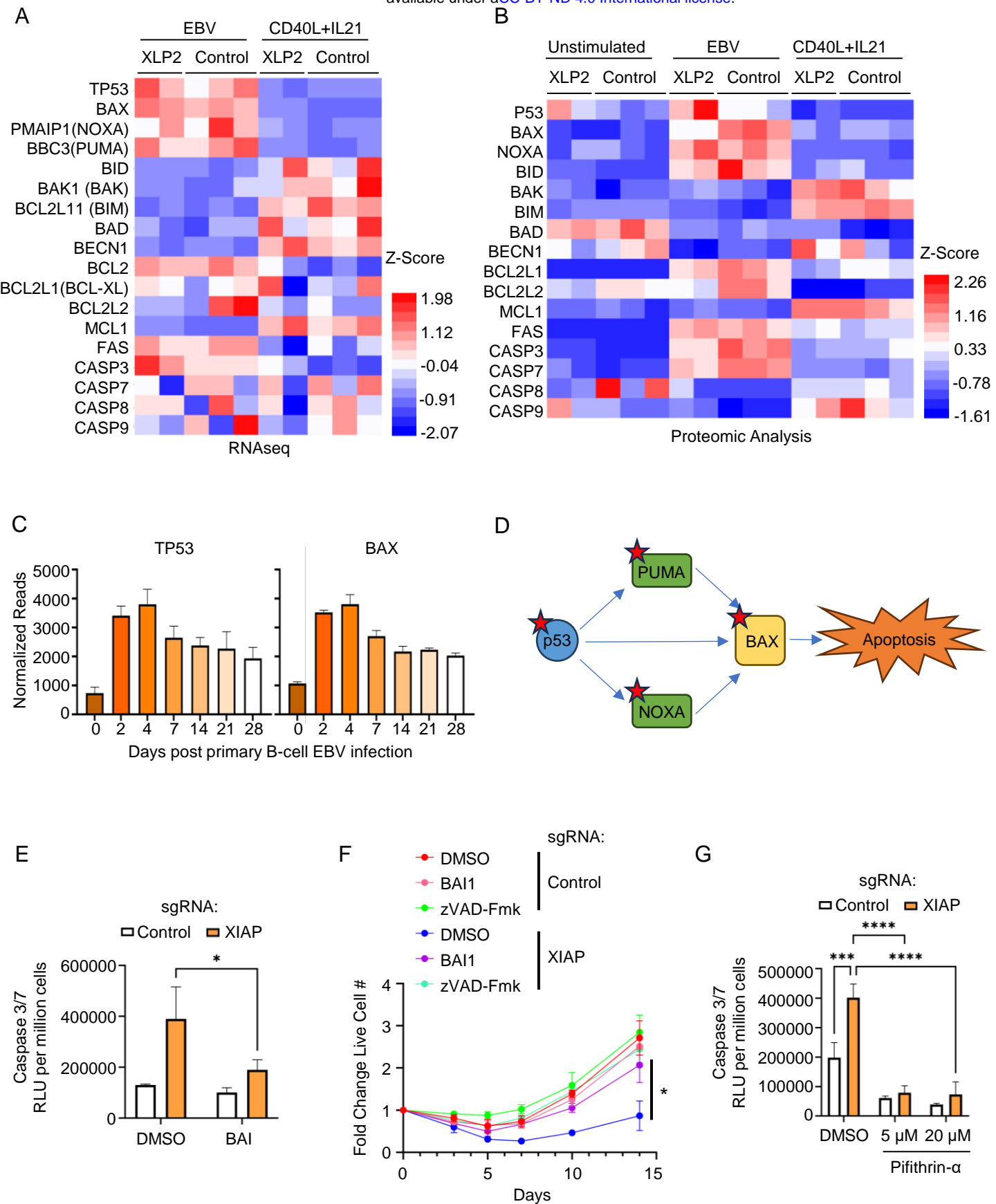
B

Proteomic Analysis

C

D

E

F

G

Figure 4. EBV but not CD40L/IL-21 activates p53- and BAX-dependent apoptosis in newly infected XIAP deficient B-cells.

(A) Heatmap of RNAseq analysis of primary B-cells from XLP2 patient or controls on Day 7-post EBV infection or CD40L/IL-21 treatment. Z-scores of normalized reads of the indicated mRNAs from n=3 replicates are shown. Columns show data from two XLP2 patients or three controls.

(B) Multiplexed tandem mass tag proteomic analysis of primary B-cells from XLP2 patients or healthy controls on Day 7 post-EBV infection or CD40L/IL-21 treatment. Unstimulated cells were harvested on Day 0. Z-scores of relative protein abundances of the indicated mRNAs from n=3 replicates are shown. Columns show data from two XLP2 patients or three controls.

(C) Mean + standard deviation (SD) TP53 and BAX mRNA expression from n=3 replicates of RNAseq analysis of primary human B-cells on the indicated days post EBV infection 33.

(D) Schematic diagram illustrating p53 that p53 target genes PUMA and NOXA can each upregulate BAX, which in turn induces the intrinsic apoptosis pathway. Red stars denote upregulation at Day 7 post-EBV infection relative to CD40L/IL-21 levels.

(E) Mean + SD caspase 3/7 activity from n=3 replicates of primary B-cells expressing control or XIAP targeting sgRNAs and treated with BAI1 (5 µM) on day 4 post EBV infection. BAI1 was added from Day 0 onwards, replenished every 3 days.

(F) Growth curve analysis of control versus XIAP edited primary B-cells and cultured with DMSO, zVAD-Fmk (20 µM) or BAI1 (5 µM) from Day 0 onwards. Mean ± SD fold change live cell numbers, relative to uninfected values, are shown. DMSO, BAI and zVAD-Fmk were replenished every 3 days.

(G) Mean + SD caspase 3/7 activity from n=3 replicates of control versus XIAP edited primary B-cells cultured with DMSO or pifithrin-α at 5 or 20 ☐M on Day 4 post-infection.

Statistical significance was assessed by two-tailed unpaired Student's t test (F) or two-way ANOVA followed by Tukey's multiple comparisons test (E and G). *p<0.05, ***p<0.001, ****p<0.0001.
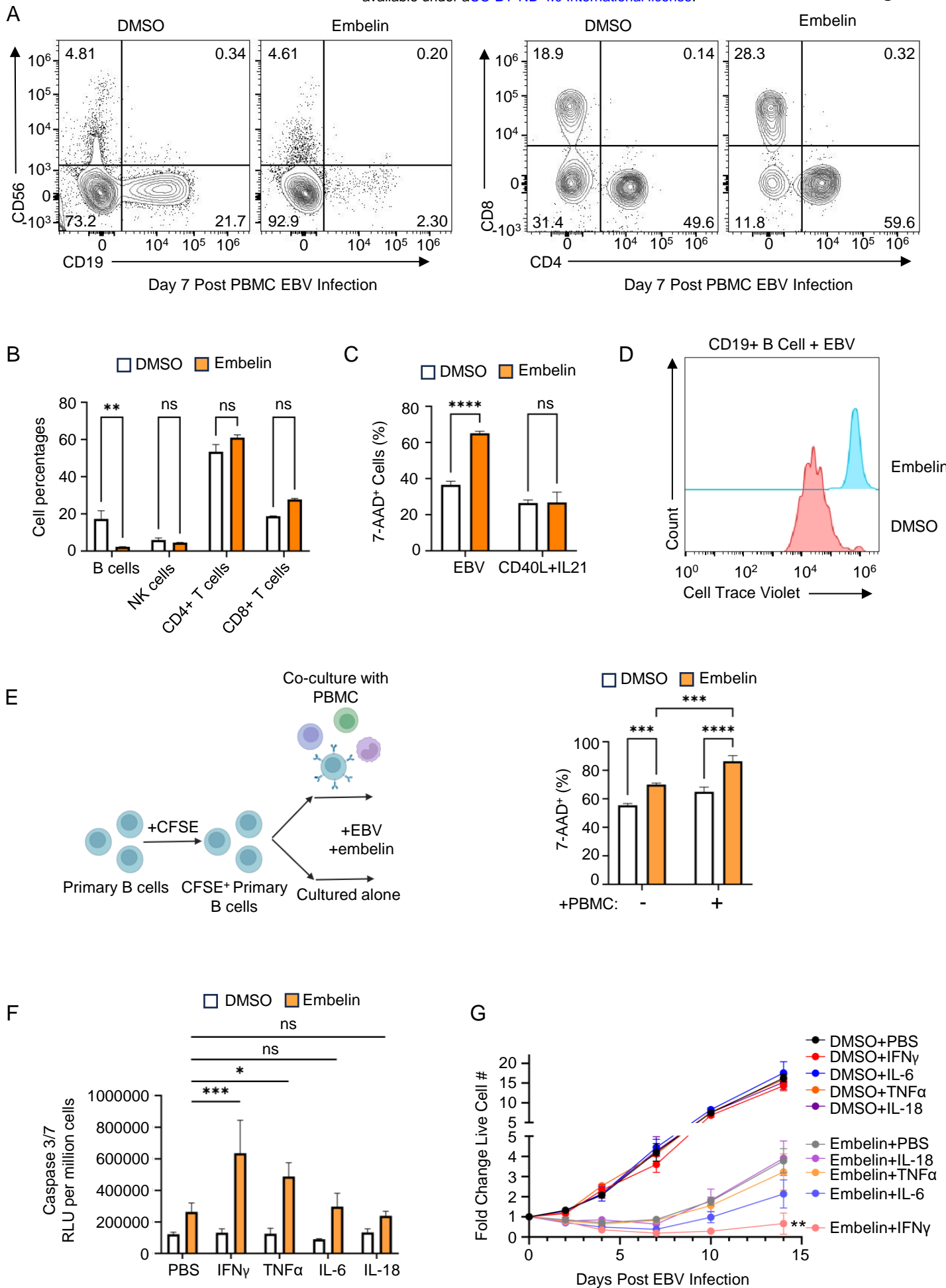
Figure 5

Figure 5. Embelin XIAP inhibition perturbs EBV-mediated primary B-cell outgrowth and sensitizes newly-infected cells to IFN□-triggered apoptosis.

(A) FACS analysis of CD4+ or CD8+ T cell, CD56+ NK cell and CD19+ B-cell subsets from PBMCs of a control donor, infected with EBV and treated with DMSO or embelin (5 μM) on Day 7 post-EBV infection. DMSO and embelin were added starting from Day 0 and replenished every 3 days.

(B) Mean + SD percentages of CD4+ or CD8+ T cell, CD56+ NK cell and CD19+ B-cells from (A) are shown.

(C) Mean + SD % 7AAD+ cells from n=3 replicates of DMSO or embelin treated primary B-cells on Day 4 post-EBV infection or CD40L/IL21 treatment. DMSO and embelin were added starting from Day 0 and replenished every 3 days.

(D) FACS analysis of CD19+ B-cells CellTrace Violet (CTV) dye dilution, whose abundance is reduced by half with each mitosis, from PBMCs treated with DMSO (control) or embelin (5 μM) on Day 7 post-EBV infection. The whole PBMC cell cultures were stained with CTV and infected with EBV and treated with DMSO or embelin (5 μM) as in (A). Cells were stained with anti-CD19 antibodies on day 7 and CTV on CD19+ B cell was analyzed. DMSO and embelin were added starting from Day 0 and replenished every 3 days.

(E) Mean + SD percentages of 7AAD+ cells of primary human B-cells from controls, cultured alone or co-cultured with autologous PBMC in the presence of DMSO versus embelin (5 μM) for 4 days. B-cells were stained with CFSE prior to PBMC co-culture, which served as a cell trace marker to allow their FACS gating within mixed PBMC cultures.

(F) Mean + SD caspase 3/7 activity from n=3 replicates of EBV-infected DMSO or embelin treated cells that were co-cultured with PBS vehicle, IFNg (50 ng/mL), TNFa (50 ng/mL), IL-6 (50 ng/mL) or IL-18 (50 ng/mL) on Day 4 post-infection.

(G) Growth curve analysis of control primary human B-cells infected by EBV and treated with DMSO or embelin (5 μM) together with IFN□, TNF□, IL-6 or IL-18 as indicated. Shown are mean ± SD fold change live cell numbers from n=3 replicates. Statistical significance was assessed by comparing each cytokine treated group with PBS control group.

Statistical significance was assessed by two-tailed unpaired Student's t test (B, C, G) or two-way ANOVA followed by Tukey's multiple comparisons test (E and F). In all experiments, DMSO, Embelin and cytokines were refreshed every 3 days. *p<0.05, **p<0.01, ***p<0.001, ****p<0.0001. ns, not significant.
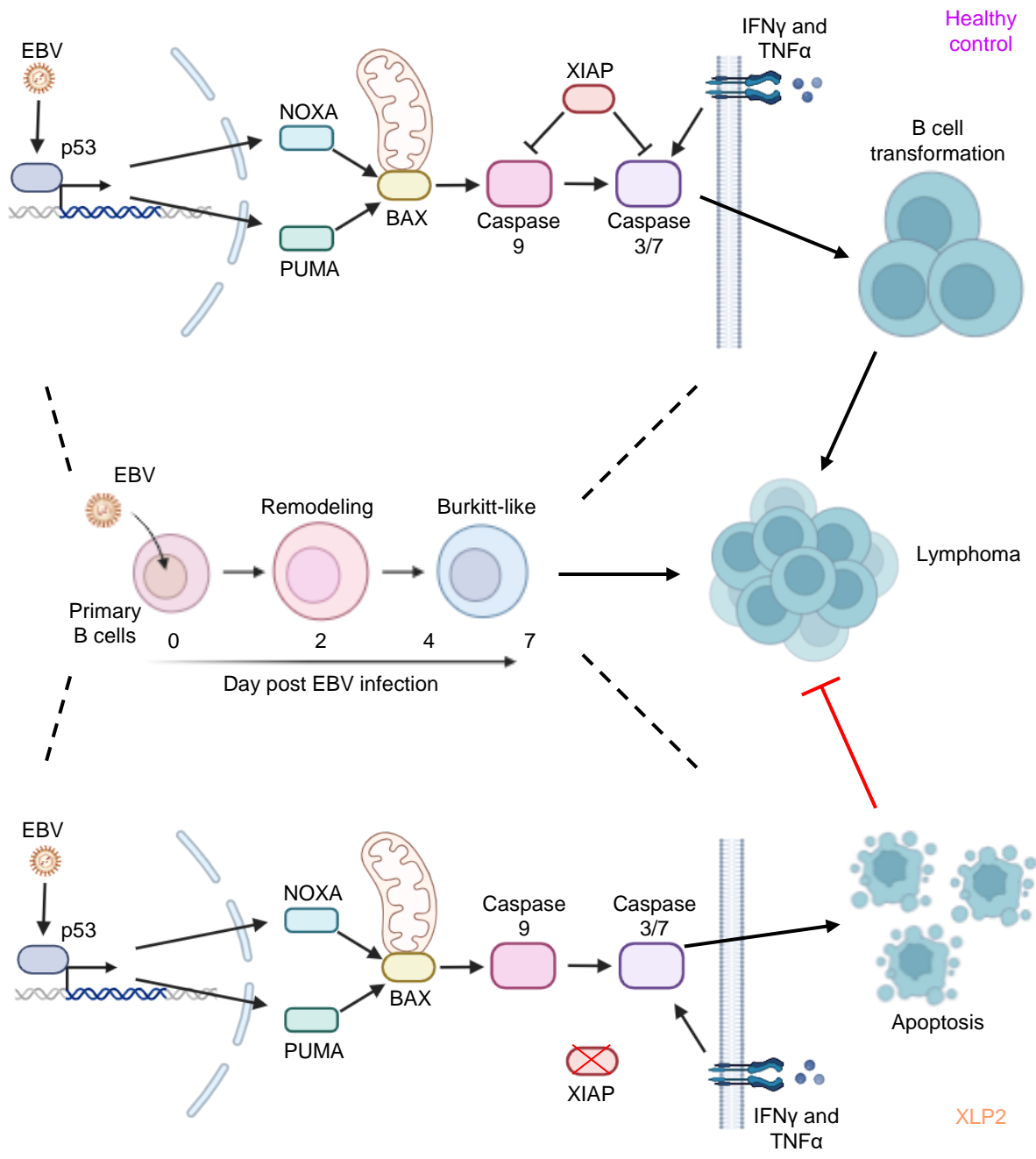
Figure 6

Figure 6. Schematic model of key anti-apoptotic XIAP role in newly EBV-infected B-cells.

EBV drives rapid proliferation of newly infected B-cells, which triggers DNA damage, upregulation of p53 and of downstream NOXA, PUMA and BAX. XIAP blocks caspase activity and apoptosis in most settings, including with XLP1, enabling newly EBV-infected B-cells to undergo transformation and in XLP1 to cause high rates of lymphomas. Lymphomas are not observed in XLP2 patients, where the absence of XIAP enables caspase 3/7 activation and apoptosis induction over the first week of EBV infection, which is exacerbated by the inflammatory cytokine milieu, in particular IFNg, restraining lymphomagenesis.